Dalton Transactions

Accepted Manuscript

ROYAL SOCIETY OF CHEMISTRY

www.rsc.org/dalton

Journal Name

RSCPublishing

ARTICLE

Binding of Copper(II) Polypyridyl Complexes to DNA and Consequences for DNA-based Asymmetric Catalysis

Cite this: DOI: 10.1039/x0xx00000x

Received 00th January 2012,
Accepted 00th January 2012

DOI: 10.1039/x0xx00000x

www.rsc.org/

Apparao Draksharapu, Arnold J. Boersma, Miriam Leising, Auke Meetsma, Wesley R. Browne* and Gerard Roelfes*

The interaction between salmon testes DNA (st-DNA) and a series of Cu(II) polypyridyl complexes, *i.e.* [Cu(dmbpy)(NO_3)$_2$] (**1**) (dmbpy = 4,4'-dimethyl-2,2′-bipyridine), [Cu(bpy)(NO_3)$_2$] (**2**) (bpy = 2,2′-bipyridine), [Cu(phen)(NO_3)$_2$] (**3**) (phen = phenanthroline), [Cu(terpy)(NO_3)$_2$].H_2O (**4**) (terpy = 2,2':6',2''-terpyridine), [Cu(dpq)(NO_3)$_2$] (**5**) (dpq = dipyrido-[3,2-d:2',3'-f]-quinoxaline) and [Cu(dppz)(NO_3)$_2$] (**6**) (dppz = dipyrido[3,2-a:2',3'-c]phenazine) was studied by UV/Vis absorption, Circular Dichroism, Linear Dichroism, EPR, Raman and (UV and vis) resonance Raman spectroscopies and viscometry. These complexes catalyse enantioselective C-C bond forming reactions in water with DNA as the source of chirality. Complex **1** crystallizes as an inorganic polymer with nitrate ligands bridging the copper ions, which adopt essentially a distorted square pyramidal structure with a fifth bridging nitrate ligand at the axial position. Raman spectroscopy indicates that in solution the nitrate ligands in **1**, **2**, **3** and **4** are displaced by solvent (H_2O). For complex **1**, multiple supramolecular species are observed in the presence of st-DNA in contrast to the other complexes, which appear to interact relatively uniformly as a single species predominantly, when st-DNA is present. Overall the data suggest that complexes **1** and **2** engage primarily through groove binding with st-DNA while **5** and **6** undergo intercalation. For complexes **3** and **4** the data indicates that both groove binding and intercalation takes place, albeit primarily intercalation. Although it is tempting to conclude that the groove binders give highest ee and rate acceleration, it is proposed that the flexibility and dynamics in binding of Cu(II) complexes to DNA are key parameters that determine the outcome of the reaction. These findings provide insight into the complex supramolecular structure of these DNA-based catalysts.

Introduction

The development of new homogeneous catalytic methods has, until recently, focused heavily on the concept of the catalytic centre, *e.g.*, a metal ion, and the control of its reactivity through the first coordination sphere, in particular tuning of the structure of ligands. Although highly successful, in particular with regard to asymmetric catalysis, recently, a paradigm shift has taken place in the fields of homogeneous catalysis and biocatalysis where the role of the microenvironment in which the catalytic centre is located is considered as a factor in determining both catalytic activity (rate enhancement) and selectivity.[1] This paradigm shift has led to new strategies in catalysis, not least directed evolution,[2] supramolecular[3] and hybrid catalysis[4] in which efforts are directed towards optimising, what is termed as, the second coordination sphere.

In DNA based asymmetric catalysis (Fig. 1), the a hybrid catalyst is formed by placing an achiral catalytically active metal complex in proximity to DNA through non-covalent interactions. Thus, the second coordination sphere provided by DNA's double helix can be harnessed directly as the source of chiral information.[5] DNA-based catalysts comprising simple 2,2'-bipyridine (bpy) and 4,4'-dimethyl-2,2'-bipyridine (dmbpy) copper complexes gave rise to very high enantioselectivities in multiple classes of C-C bond forming reactions. An intriguing observation is that the ee's were significantly higher than those obtained using other copper(II) complexes with ligands such as phenanthroline (phen), dipyrido-[3,2-d:2',3'-f]-quinoxaline (dpq) and dipyrido[3,2-

a:2',3'-c]phenazine (dppz). Furthermore, using copper complexes of 2,2':6',2''-terpyridine (terpy), the opposite enantiomer of the products was obtained in excess, albeit that the reactions were generally much slower.[5g] What is striking is that the presence of DNA was found to cause an additional acceleration of the reaction compared to the reactions catalysed the copper(II) complexes alone, without DNA.[5d] These DNA-induced rate accelerations differed depending on the copper complex used and ranged from ~2-fold in case of Cu(II)bpy and Cu(II)phen, to a surprising ~60 fold in case of Cu(II)dmbpy.

A key challenge in developing a mechanistic understanding of these complex supramolecular catalyst systems is to identify at a molecular level the precise mechanism by which the chiral information contained within the structure of DNA is transferred in such a highly efficient manner to the product of, *e.g.*, copper(II) catalysed reactions. In the first instance the binding mode of the kinetically competent complex to DNA needs to be established, in order to understand how such interactions are affected by the presence of the copper(II) binding substrates (*e.g.*, aza-chalcones) under conditions where catalysis takes place. Perhaps surprisingly, the nature of binding of such simple complexes, *e.g.*, Cu(II)bpy, to DNA is unknown to date.

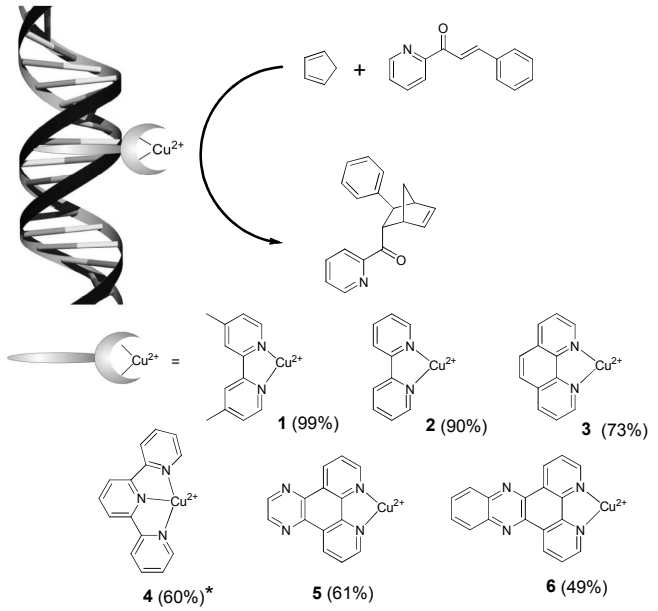

Fig. 1 Cu(II) complexes **1** - **6**. The enantioselectivity obtained in an asymmetric Diels-Alder reaction between azachalcone and cyclopentadiene -reported previously is shown in parentheses (*for complex **4**, the opposite enantiomer was obtained).[6]

Elucidating the interaction between metal complexes, substrates and drugs with double stranded DNA is an area of intense interest.[7] Definitive assignment of the binding mode of the compounds with DNA is necessary, for example, in the development of new chemotherapeutic agents.[8] However, long chain biomolecules such as DNA are inherently inhomogeneous environments in which to embed small molecules. A range of spectroscopic techniques have been employed to probe small molecule-DNA interactions including X-ray crystallography,[9,10] UV/Vis absorption,[10] Circular and Linear Dichroism,[11,16c] EPR,[12] Fluorescence[13] and NMR spectroscopy[14] together with viscometry[15] and DNA melting curves, to name but a few. A key challenge in assigning the mode by which compounds bind to DNA is that limited data sets can often lead to incorrect assignments, due to the ambiguity and exceptions-to-the-rules encountered with each technique employed to address this question. For example, the complex $[Ru(phen)_3]^{2+}$ shows characteristics of intercalation, as well as groove binding, to DNA.[17] Hence, data from spectroscopic and the other techniques can present a confused picture as to the overall binding, depending on the dominance of contributions from each binding mode to the data obtained with a particular technique.[11b,16] Hence, in studying such systems, achieving the spectroscopic sensitivity and discrimination between not only bound and unbound species, but also species bound in distinct local environments is a key challenge. Barton et al. have proposed criteria for the assignment of the binding interactions (*e.g.,* intercalation) of compounds to DNA, in which a multi-technique approach is promulgated and the potential conflict between data obtained with distinct techniques regarding binding mode is recognised.[17]

In this contribution we report a spectroscopic study of the interaction of st-DNA with the Cu(II) complexes $[Cu(dmbpy)(NO_3)_2]$ (**1**), $[Cu(bpy)(NO_3)_2]$ (**2**), $[Cu(phen)(NO_3)_2]$ (**3**), $[Cu(terpy)(NO_3)_2].H_2O$ (**4**), $[Cu(dpq)(NO_3)_2]$ (**5**) and $[Cu(dppz)(NO_3)_2]$ (**6**). These complexes have proven to be versatile catalysts especially for asymmetric C-C bond forming reactions in water with DNA as the source of chirality.[1a] UV/Vis absorption, Circular Dichroism, Linear Dichroism, EPR, Raman spectroscopy and viscometry were employed to elucidate the binding mode or modes by which these complexes interact with st-DNA. UV resonance Raman spectroscopy in particular proves useful in the case of complexes **5** and **6** where shifts to lower wavenumbers are observed for certain modes, a previously unreported phenomenon that is consistent with intercalation.[18] For complexes **1** and **2**, by contrast, the combined spectroscopic data demonstrate that the interaction between these complexes and st-DNA can be broadly characterised as groove binding, whereas complexes **3** and **4** show spectroscopic characteristics suggestive of both groove binding and intercalation, with the latter dominating. The main goal of this contribution is to investigate the DNA binding modes of the Cu(II) complexes **1** - **6** and their relation to the enantioselectivities in the DNA-based catalytic asymmetric Diels-Alder reactions reported previously.[6]

Results

Synthesis and characterization of Cu(II) complexes

Complexes **1**, **2**, **3**, **5** and **6** (Fig. 1) were obtained according to literature procedures[6,18] and were characterized by elemental analysis, FTIR, EPR, Raman and resonance Raman

spectroscopy (see ESI for details). For **4**, mixing of terpy with $Cu(NO_3)_2 \cdot 3H_2O$ in ethanol resulted in the formation of a green powder, with the structure $[Cu(terpy)(NO_3)_2].H_2O$ (**4**) indicated by elemental analysis, FTIR and Raman spectroscopy. Raman and FTIR spectroscopy show that coordination to the Cu(II) ion results in a shift in the pyridyl modes of the ligands at ca. 1600 cm^{-1} to higher wavenumbers (see ESI section 6 for details).

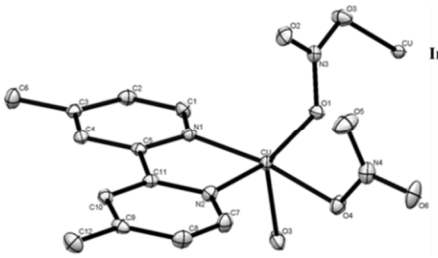

Fig. 2 Structure of **1** at 50% probability ellipsoids (left) and selected bond lengths (right). Hydrogen atoms are omitted for clarity. CCDC 960057

Blue crystals of **1** were obtained by mixing a solution of dmbpy with $Cu(NO_3)_2 \cdot 3H_2O$ in ethanol followed by standing in an ethyl acetate bath. **1** crystallised as a polymer with a nitrate ligand bridging between Cu(II) ions. The formally penta-coordinate Cu(II) ions have a distorted square pyramidal structure with a highly elongated Cu-O bond (2.35 Å) in an axial position (Fig. 2). The nitrogen atoms of the ligand dmbpy and the oxygen atoms of two nitrate ligands bind to the Cu(II) ion with bond lengths of ca. 1.98 Å.[19] A dihedral angle of 5º is observed between the pyridine rings in the dmbpy ligand. The distances between O2 and O5 and Cu are 2.82 and 2.77 Å, respectively, and are too long to be considered as bonding.[19]

EPR Spectroscopy

The EPR spectra of **1 - 4** show four parallel peaks ($g_{\|}$) and one perpendicular peak ($g_{\perp}$), Fig. S23. For **1**, the axial symmetry observed, $g_{\|}>g_{\perp}>2.0023$, indicates that the highest occupied orbital is the $d(x^2-y^2)$ orbital. Furthermore, $g_{\|}/A_{\|}$, a factor influenced by the geometry and the donor atoms,[20] is characteristic of slightly distorted square planar complexes; in agreement with the X-ray structural analysis. The superhyperfine structure in the perpendicular axis shows five signals as expected with two nitrogen atoms (2N+1) coordinating the Cu(II) ion, indicating that as in the solid state, in solution each Cu(II) ion is coordinated to a single dmbpy ligand.

The EPR spectrum of **1** in the presence of st-DNA is similar to that in its absence with an additional, albeit, a weaker set of signals from a new species, indicating that two populations of complex were present - *e.g.* **1** and **1** bound to st-DNA (Fig. 3). The dependence of the EPR spectrum of **1** on the presence of various short strand DNA-sequences, was examined also. In the presence of self-complementary oligonucleotides containing various DNA sequences the parallel peaks in the EPR spectrum of **1** shift to higher field compared to shifts observed with st-DNA (Table 1 and Fig. 3). With the synthetic duplexes $d(GACTGACTAGTCAGTC)_2$ and $d(TCAGCGCGCTGA)_2$ only one set of parallel peaks was observed, while with $d(TCAGGGCCCTGA)_2$ several overlapping sets were observed; suggesting the presence of multiple distinct copper complexes in the latter case.

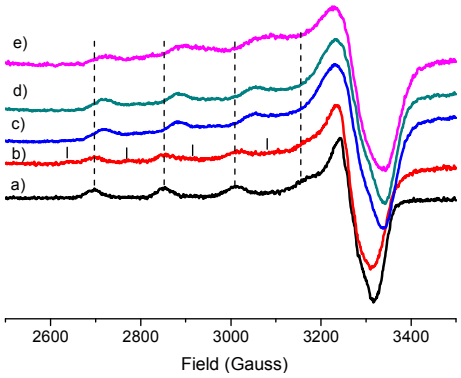

Fig. 3 X-band EPR of **1** in buffer (20 mM MOPS pH 6.5, 1.8 vol% DMSO), and in the presence of st-DNA. Experimental conditions: T = 77 K; Microwave frequency = 9.46 GHz; microwave power = 20 mW; 10 G field modulation amplitude; time constant 81.92 ms; conversion time 81.92 ms; 3 accumulations. 9 accumulations in the case of c - e. a) 0.3 mM **1**. b) 0.3 mM of **1** and 1.4 mg/mL st-DNA, c) 0.25 mM of **1**, 1.2 mg/mL $d(TCAGCGCGCTGA)_2$, d) 0.25 mM of **1**, 1.2 mg/mL $d(GACTGACTAGTCAGTC)_2$ and e) 0.25 mM of **1**, 1.2 mg/mL $d(TCAGGGCCCTGA)_2$.

Table 1 EPR data for **1** at 77 K.[a]

Conditions	$g_{\|}$	$g_{\perp}$	$A_{\|}$ ($\times 10^{-4}$ cm^{-1})	$A_{\perp}$ ($\times 10^{-4}$ cm^{-1})	$g_{\|}/A_{\|}$
EtOH:buffer (2:1)	2.32	2.07	154	14	151
Buffer	2.31	2.07	158	15	146
with st-DNA	2.30	2.07	160	-	144
[c](minor species)	*2.38*	*2.07*	*161*	-	*148*
with 12mer-DNA[b]	2.28	2.07	165	-	138

[a]See Fig. S23 for details. [b]12mer-DNA = $d(TCAGCGCGCTGA)_2$.[c] Values are approximate due to lower S/N ratio.

The EPR spectra of **2** and **3** (Fig. S23) show four parallel signals ($g_{\|}$) and one perpendicular signal ($g_{\perp}$) as for **1**.[21] In contrast to **1**, the additional features due the presence of st-DNA were less pronounced. The EPR spectrum of **4** (Fig. S23) shows three parallel signals along with unresolved superhyperfine splitting. The parallel peak at ~3140 G lies under the perpendicular signal. In contrast to **1**, addition of st-DNA to **4** does not lead to the appearance of additional features (Fig. S24).

Raman Spectroscopy

Raman spectroscopy shows considerable potential as a tool in studying small molecule-DNA interactions.[22] Although routine assignment of the binding modes of substrates to DNA based on Raman spectroscopic data has not been established to date, Kelly *et al.*[23] and Barton *et al.*[24] have described the effect of intercalation to calf thymus DNA on $[Ru(phen)_2(dppz)]^{2+}$ using time resolved and continuous wave resonance Raman spectroscopy, respectively. However, in those studies shifts in the Raman bands of the potential DNA binding moieties themselves were not observed in the presence of st-DNA. The

overlap between the absorption spectrum of st-DNA and the complexes in the UV region required that a resonance Raman study of st-DNA was carried out also in order to establish contributions to the spectrum from st-DNA in the spectra obtained with the complexes. A detailed discussion of which can be found in the ESI, section 6.

In the presence of st-DNA the resonance Raman spectra of complexes **1** - **4** are essentially identical to those obtained in its absence, with the exception of the presence of bands due to st-DNA itself. Importantly significant shifts in peak positions were not observed (*vide infra*). The resonance Raman spectra recorded at λ_{exc} 355 nm of **1** in the absence and presence of st-DNA are shown in Fig. 4a.

Dpq and dppz are well-known intercalators of DNA.[18] For metal complexes such as $[Ru(phen)_2(dppz)]^{2+}$, the presence of ct-DNA results in a decrease in the intensity and broadening of the Raman bands, at λ_{exc} 355 nm, of the dppz ligand. To the best of our knowledge, changes in peak positions in the Raman spectra of those complexes when they bind to DNA have not been reported. Intercalation of a ligand/complex into st-DNA could have a significant effect on band position of the ligand if the interaction leads to a change in its conformation or electron density, as noted for several drug-like compounds where a shift to lower wavenumber for several bands has been observed upon intercalation.[22d]

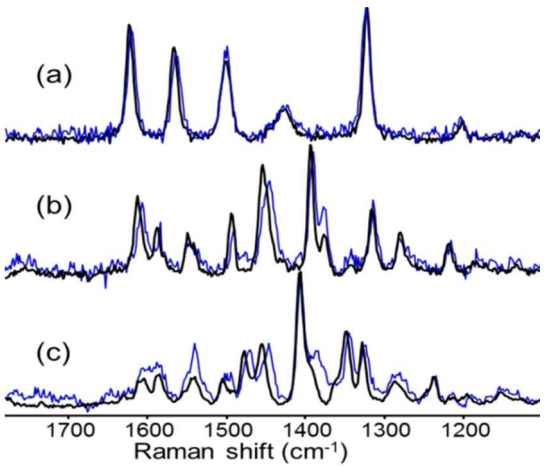

Fig. 4 Raman spectra of (a) **1**, (b) **5** and (c) **6** in the presence (thin blue line) and absence (thick black line) of st-DNA at λ_{exc} 355 nm. Raman spectra were solvent subtracted followed by a multipoint baseline correction (contributions from DNA were removed by scaled spectral subtraction).

Shifts in the Raman spectra were not observed in the case of **1** and **5** with 150 mM sodium dihydrogen phosphate (Fig. S33-35), suggesting that the phosphate backbone of DNA is not involved in coordination (*vide infra*). The resonance Raman spectra of complexes **1** - **4** in the absence and presence of st-DNA are essentially identical with the exception of bands due to st-DNA (Fig. S32). Significant shifts in peak position were not observed. By contrast, for **5** and **6**, several bands are shifted by several cm^{-1} to lower wavenumber (Fig. 4).[25] Overall the Raman data indicate that π-π stacking interactions lead to a decrease in the band gap between π→π* orbital of the ligand and base pairs, which is consistent with the substantial bathochromic shift in the absorption spectra observed upon addition of st-DNA to **5** or **6** and, hence, intercalation can be inferred from these data (*vide infra*).[17]

UV/Vis absorption spectroscopy

UV/Vis absorption spectroscopic data for complexes **1** to **6** in the presence and absence of st-DNA are summarised in Table 2 and Fig. 5 (and Fig. S29-31). For complexes **1** to **6**, π→π* transitions are observed between 290 - 400 nm with a red shift in the λ_{max} from 310 nm to 380 nm as the extent of conjugation in the ligand increases from phen to dppz. The binding constants (10^3 to 10^5 M^{-1}) for **1** - **6** with st-DNA were reported earlier.[6] Complexes **1** - **4**, show similar binding affinities, while **5** and **6** show 10 and 100 times higher binding constants, respectively.

Table 2 UV/Vis absorption data and binding constants for complexes **1** - **6**.

	λ_{max} (nm)	λ_{max} (nm) (with DNA)	% hypochromism	binding affinity $(M^{-1})^a$
1	297 307	--- 307	--- 33 (307)	1.12 (± 0.02) x 10^4
2	300 310	300 310	--- 14 (310)	9.4 (± 0.3) x 10^3
3	295, 327 (w), 345 (w)	----	---	1.3 (± 0.1) x 10^4
4	313 (sh) 326 339	--- 332 339	--- 34.3 (326) 28.4 (339)	5.9 (± 0.1) x 10^3
5	309 (sh) 321 335	314 (sh) 326 340	--- --- 12.3 (335)	7.2 (± 1.2) x 10^4
6	325 359 377	331 363 381	--- --- 48.5 (377)	8.0 (± 3.0) x 10^5

sh (shoulder), w (weak). Conditions as described in the caption of Fig. 5. [a] binding constants were taken from Ref. 6 and in the case of **1** the binding affinity value is an average of the multiple binding species (*vide infra*).

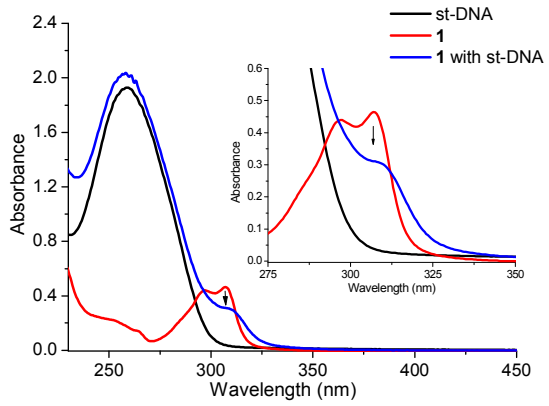

Fig. 5 UV/Vis absorption spectra of complex **1** (0.03 mM) in the absence and presence of st-DNA (0.13 mg/mL). The ratio of the copper complex to DNA base pairs is 1:6. st-DNA in Milli-Q water.

For **1** and **2**, negligible bathochromic shift, hypochromism and band broadening is observed upon addition of st-DNA. The effect of st-DNA on the absorption spectrum of **3** was not easily discerned due to overlap with the absorption of st-DNA itself.

For **4**, the band at 326 nm underwent a bathochromic shift of 6 nm, however, the absorption band at 339 nm does not shift; both bands show hypochromism. For **5**, st-DNA induced a 5 nm bathochromic shift for the bands between 309 and 335 nm, with minor hypochromism, which is surprising considering the higher binding affinity of **5** with st-DNA (*vide infra*). The absorption bands of complex **6** at 359 and 377 nm were shifted bathochromically by 4 nm upon addition of st-DNA, however, a greater hypochromic effect was observed compared with that of **5**.

Circular Dichroism (CD) Spectroscopy

CD spectroscopy was employed to explore the interaction of the copper complexes with st-DNA through observation of induced CD (ICD) in the complexes. The CD spectra of st-DNA in the absence and presence of the achiral copper complexes are shown in Fig. 6 and Fig. S38. For **1** and **2**, ICD bands of similar intensities were observed at 302, 312 nm and 304, 314 nm, respectively. The positive CD band of st-DNA at 280 nm shows a slight decrease in intensity in the presence of **1**, and to a lesser extent, **2**. The decrease is likely to be due to a negative ICD band for the complexes in this region (Fig. 6). Notably, the terpyridine based complex **4** shows at most a very weak ICD effect.

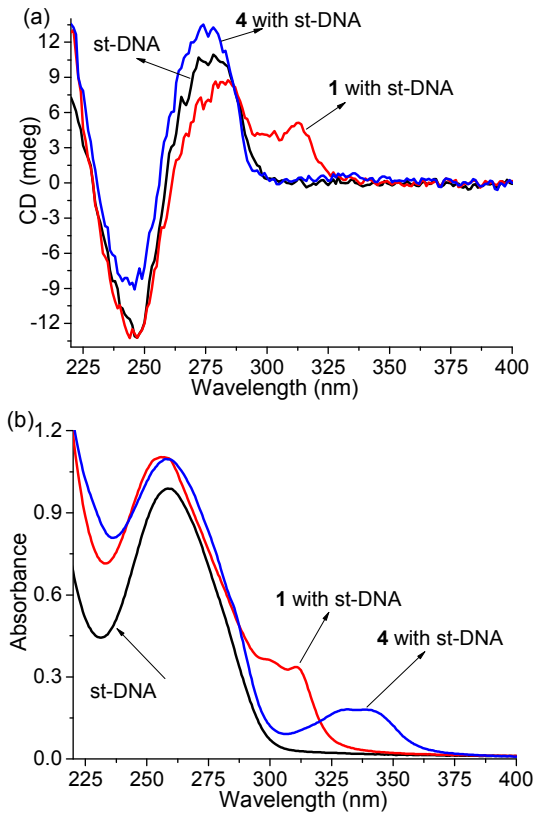

Fig. 6 (a) CD and (b) UV/Vis absorption spectra of **1** and **4** in the presence of st-DNA. Conditions: ratio of the Cu complex to DNA base pairs is 1:6. st-DNA (0.065 mg/mL), Cu complex (0.015 mM) in Milli-Q water.

The CD spectrum of st-DNA in the presence of **3** shows a positive ICD at ca. 280 and 300 nm and a slight shift in the negative band at ca. 260 nm, which correspond to the main absorption bands of the complex. For both **5** and **6** the positive CD band of st-DNA appears to increase in intensity by about 50% whereas the negative band becomes ca. 25% weaker. The changes correspond to changes in the corresponding UV absorption bands for both complexes. For **5**, ICD bands corresponding to absorption at wavelengths greater than 300 nm were not observed, while for **6**, a negative ICD band at 290 nm was observed upon addition of st-DNA.

Effect of ionic strength on binding to DNA and catalysis

Intercalation and groove binding involve both hydrophobic and electrostatic/hydrogen bonding interactions where the DNA binding species is cationic. Indeed for cationic complexes electrostatic interactions with the negatively charged DNA would be expected to be important, especially for groove binding. This interaction can be diminished by screening the negative charge of the DNA backbone with a large excess of Na^+.[26] The effect of chloride and phosphate ions on complexes **1** and **5** was examined in the absence of st-DNA. Addition to 150 mM of NaCl to solutions of **1** and **5** resulted in a red shift of the d-d band by 25 nm and 3 nm, respectively. Interestingly, peak shifts in the resonance Raman spectra were not observed. In contrast to NaCl, addition of NaH_2PO_4 (150 mM) to **1** and **5** gave rise to hypochromism along with a blue shift in the d-d band by 3 nm and 26 nm, respectively (Fig. S36). The EPR spectra of these complexes were strongly affected by the presence of sodium dihydrogen phosphate (Fig. S37), indicating that phosphate coordinates to copper(II). The EPR spectrum of **1** in the presence of a large excess of NaH_2PO_4 (Figure S37) is typical of that of a π-π stacked Cu(II) dimer,[27] however, such EPR signals are not observed for **1** in presence of st-DNA.

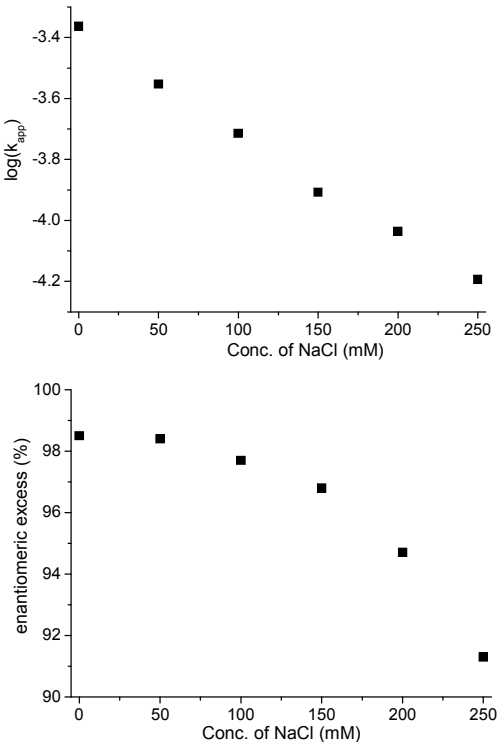

Fig. 7 Effect of NaCl on reaction rate (k_{app}) and enantiomeric excess of the product in the **1**/st-DNA catalysed Diels-Alder reaction between azachalcone and cyclopentadiene.[6] Conditions: ratio of **1** to base pairs DNA is 1:6 st-DNA (1.4 mg/mL), **1** (0.3 mM), azachalcone (1 mM) and cyclopentadiene (15 mM) in MOPS buffer (20 mM, pH 6.5) at 5 °C.

The electrostatic contribution to binding of the complexes to st-DNA was investigated by titration of the metal complexes with st-DNA in the absence and presence of NaCl (100 mM). The binding affinity of **1** and **2** decreased to such an extent that it was no longer possible to quantify binding by UV/Vis absorption spectroscopy. The addition of 50 mM NaCl results in a complete change to the EPR spectrum of **1** (Fig. S37),[28] indicating that addition of NaCl results in formation of a (dmbpy)copper(II)(chloride) species.[29] Furthermore, the coordination of chloride to copper(II) will shift the equilibrium to a neutral (dmbpy)copper(II) chloride complex thereby reducing the effective overall concentration of **1** (both unbound and DNA bound, see scheme 1). In the case of **5**, the binding affinity decreased modestly in the presence of NaCl (100 mM) from 7.2×10^4 to 1.3×10^4 M^{-1}.

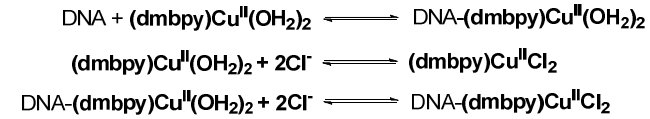

Scheme 1 Equilibria established in solution in the presence of NaCl, DNA and **1**.

The decrease in binding affinity of **1** to st-DNA upon addition of NaCl was found to correlate with the outcome of the catalysed Diels-Alder reaction: increasing the concentration of NaCl led to a decrease in both the rate and the enantioselectivity of the reaction (Fig. 7). These changes can be consistent the decrease in the proportion of **1** bound to st-DNA, and hence an increase in the concentration of unbound complex **1** in solution; the unbound species will catalyse the reaction in a racemic fashion albeit at a much lower rate.[5b]

Both the reaction rate and the enantioselectivity in the copper(II) catalysed Diels-Alder reaction studied were found to decrease as the concentration of NaCl increased. If the effect of NaCl was only to reduce the overall concentration of **1** in solution, through formation of a non-catalytically active copper(II) chlorido species, then this would affect the observed reaction rate but not the enantioselectivity achieved. Since a drop in ee is observed also, it may be concluded that the equilibrium between DNA bound and unbound complex **1** must be affected by addition of NaCl, from which it could be inferred that there is a significant electrostatic component to the binding of **1** to DNA.

Linear Dichroism (LD) Spectroscopy

Linear Dichroism (LD) spectroscopy was employed to gain insight into the alignment (and hence binding mode) of the various copper complexes with respect to the helix axis of st-DNA using sheer induced alignment in a micro-Couette cell.[30] For **1**, a negative rLD (reduced LD) signal indicates that the angle with which the plane of the dmbpy ligand aligns with the axis of the st-DNA helix is ~65º, which is intermediate between that expected for intercalation (ca. 90º) and minor groove binding (ca. 45º) and is close to that reported for Δ-$[Ru(phen)_3]^{2+}$, which binds via several binding modes, with an average angle of 70º (Fig. 11). In the case of **2**, an angle of 55º was determined, indicating that **2** engages in groove binding with st-DNA. It is of note that William *et al.*[12] have suggested an angle of ~40º between the $g_{||}$ axis of Cu^{II}(bpy) and long axis of the DNA helix, which is close to the 55º determined in the present case. For **3** and **4**, a strong negative rLD signal was observed with angles of 76º and 79°, which are close to that expected for intercalation (Fig. S39 and S40),[31] and consistent with the $g_{||}$ axis of Cu^{II}(phen) being parallel to the DNA-fibre axis as proposed by William *et al.*[12]

Effect of complexes 1 - 5 on the viscosity of st-DNA containing solutions

The binding of small molecules to st-DNA can result in a change in viscosity,[32] due to partial unwinding of the helix to accommodate intercalators thereby increasing the hydrodynamic radius of st-DNA. For groove binders the helix, and hence the hydrodynamic radius, is relatively unperturbed and therefore only minimal changes in viscosity are expected. For complexes **3**, **4** and **5** the viscosity of the solution increased to a significant extent in comparison to complexes **1** and **2** (Fig. S41).

Discussion

In the present study the conditions employed in this study are comparable to those used in the catalysis reported previously.[5] Addressing the question as to the mode by which the complexes

bind st-DNA, even before addition of substrate, presents a challenge as no single technique can distinguish between specific binding modes, *e.g.*, intercalation, groove binding, unambiguously.[17] This point has been demonstrated, for example, with regard to UV/Vis absorption spectroscopy. Although intercalators generally give rise to significant red shifts upon binding to DNA, which are not typically observed in the case of groove binders, examples of groove binders have been reported that undergo significant red shifts upon binding DNA as well.[33] Indeed in the present study, it was found that for all complexes a decrease in absorbance and band broadening is observed upon addition of st-DNA together with a small to substantial bathochromic shift in the lowest energy absorptions. Hence, UV/Vis absorption spectroscopy alone cannot provide a definitive answer, albeit that for complexes **5** and **6**, which contain ligands expected to intercalate,[18] the changes are somewhat more pronounced than for the other complexes.

Evidence for groove binding to DNA by complexes 1 and 2.

For complex **1** and **2** the changes observed in the UV/Vis absorption spectra upon addition of st-DNA are ambiguous with regard to assigning binding mode as they can be interpreted both as being characteristic of intercalation and of groove binding.[17] Intercalation would be expected to result in a larger bathochromic shift, however, the absence of change is in itself not conclusive. An important observation is that although the proportion of the complex bound to DNA, under catalytically relevant conditions, is higher than that unbound, the (resonance) Raman spectra of the complexes are unaffected by the presence of st-DNA (*vide infra*). In the case of **1**, for which the solid state structure has been determined, apart from exchange of NO_3^- ligands with H_2O, the solid state structure of the complexes (*i.e.* pseudo square planar) can be assumed to be retained in solution based on non-resonant Raman spectroscopy. However, in the presence of sodium chloride or sodium dihydrogen phosphate at high concentrations it is apparent that both ions compete with water to bind to the copper(II) ions.

Previously, it was noted that the melting temperature of st-DNA is unaffected by addition of **1**.[5d] In the present study a modest increase in the viscosity of a DNA containing solution, together with broadening of the UV/Vis absorption spectrum, is observed upon addition of **1** or **2**. A strong ICD signal was observed at wavelengths where **1** and **2** absorb and the negative rLD signal indicates an angle of 65º and 55º, respectively, between the axis of the DNA helix and the plane of the complex. In addition, room temperature EPR studies in a flow cell where partial alignment of the DNA occurs indicates that the binding of **1** and **2** is relatively static on the EPR time scale (see section 8 of ESI). Even though the slight increase in viscosity and the bathochromic shift in the lowest energy UV absorption bands are indicative of intercalation, overall it is concluded from the melting temperature, rLD, and UV resonance Raman spectroscopy that **1** and **2** interact with st-DNA through groove binding.

The effect of st-DNA on the spectroscopic characteristics of **1** are overall similar to those for **2**. A key difference, however, is in their EPR spectra. An additional weaker signal was observed in the case of **1** in the presence of st-DNA, suggesting that complex **1** is bound in at least two distinct ways. For **2**, the presence of DNA did not affect the EPR spectrum. The relevance of the additional species observed by EPR to catalysis is not clear, as the solution was frozen at 77 K, and the spectra in the absence of substrate, which will compete for copper(II) coordination sites. In the case of synthetic oligonucleotides a new copper(II) species was observed by EPR spectroscopy, possibly due to coordination moieties of DNA bases to copper. This relates to the observation that the DNA melting temperatures of these duplexes decreased in the presence of **1**.[5d] The EPR spectrum of **1** in the presence of the duplexes does not coincide with the additional features in the presence of st-DNA, whereas the catalytic activity and selectivity are comparable, indicating that the additional species in case of the duplexes is not likely to be of relevance to the result of catalytic reaction.

Evidence for intercalation as the major binding mode for complexes 3 and 4

Complexes **3** and **4**, although structurally distinct, show similar effects of binding to DNA spectroscopically. For **3**, the effect of st-DNA on the absorption spectrum was not easily apparent due to substantial overlap with the absorption spectrum of st-DNA. However, an ICD signal at 300 nm was observed. In the case of **4**, a 7 nm bathochromic shift and 34% hypochromism in the absorption of the complex, and a very weak, if any, ICD was observed. As for **1** and **2**, addition of st-DNA has no effect on the resonance Raman spectrum of **3** and **4**. LD spectroscopy indicates an average angle of 74º between DNA helix axis and phenanthroline ligand of **3**, and an average angle of 78º between the plane of the terpy ligand of **4** and the DNA helix axis. The angles determined are closer to those expected for intercalators (*i.e.* 90º). These observations, in combination with the increase in viscosity of a solution of st-DNA upon addition of **3** or **4**, point towards intercalation as the major binding mode. It should be noted, however, that similar ambiguities in the data were encountered in the assignment of the binding mode of $[Ru(phen)_3]^{2+}$ to DNA.[16] Nevertheless, even though the binding mode of **3** and **4** is assigned as intercalation, the possibility that groove binding takes place also cannot be excluded entirely. Moreover, the binding mode is likely to be dependent on the local DNA sequence.[16]

Evidence for DNA intercalation of complexes 5 and 6

Complexes **5** and **6** are based on the planar 1,10-phenanthroline core and, a priori, intercalation is expected to contribute substantially to the binding of these complexes with st-DNA, since complexes of the ligands dpq and dppz are indeed well known intercalators.[18] The spectroscopic and physical data obtained for **5** and **6**, *i.e.* the batho- and hypo-chromaticity, negative ICD and rLD of 90º and notably the shifts observed in the resonance Raman spectra (which are not observed with

complexes **1** - **4**), lead to the conclusion that these complexes, primarily, intercalate into st-DNA.

The DNA binding mode in DNA-based asymmetric catalysis

The determination of the DNA-binding mode of the complexes allows for comparison with the data from DNA-based asymmetric catalysis. Complexes **1** and **2** provide the highest ee's in DNA-based asymmetric catalysis, *i.e.* 99% and 90% respectively, and these complexes appear to bind DNA by groove binding. Complex **3** tends to undergo intercalation in comparison to **1** and **2**, and provides ee's of ca. 73%. Complexes **5** and **6** intercalate predominantly and provide the lowest ee's of 61 and 49%. From this it is tempting to conclude that a relation between the binding mode and ee obtained exists. However, other parameters, which might be related to the DNA-binding mode, such as the binding affinity of the complexes to the DNA, also track the trend of the ee. Another parameter which might influence the ee could be the rate at which the complex shifts between sites and binding modes with DNA: binding in a one particular manner to DNA may result in higher activity and selectivity compared to other arrangements, and when a complex is unable to sample these most active and selective pockets, for example because it is bound in a conformationally unfavourable manner, it will result in a reduced overall ee.

Previously we have shown that the ee achieved correlates with reaction rate for a series of different DNA sequences. Comparison of the binding of **1** to short strand DNA sequences using EPR was complicated by the formation of an additional species, which is unlikely to contribute to catalysis, and can even be an artefact due to freezing or the absence of substrate. Nevertheless, the data highlights the fact that complex **1** can have multiple coordination environments, as postulated previously.

Complex **4** generates the opposite enantiomer in DNA-based asymmetric catalysis. Here it is shown that the binding mode is more comparable to that of **3**, and hence, the binding mode per se is not determining enantiomeric preference in an obvious manner. This finding is consistent with the hypothesis that it is the coordination geometry of the substrate to the copper that ultimately determines enantiopreference.[5g]

To summarise, to understand the mechanism of stereo-control the DNA-binding mode, *i.e.* the structure of the chiral microenvironment provided by the DNA in which catalysis takes place is crucial. Indeed, differences in binding fashion are partially reflected in the differences in ee obtained in DNA-based asymmetric Diels-Alder reactions. However, the available data suggests that the flexibility in binding mode combined with the dynamic binding, which was suggested by the room temperature EPR studies, are key parameters to achieve high enantioselectivities in catalysis. For example **5** and **6** are intercalating, which means that the DNA binding is static. This reflected in the lower ee's obtained in the reaction the catalysed reaction. In contrast, **1** and **2** can bind DNA in multiple binding modes and orientations, thus allowing the complex to adopt a more favourable orientation in the DNA upon binding of the substrate. In other words, the DNA-based hybrid catalyst has the potential to adjust its structure upon binding of the substrate, reminiscent of the induced fit model proposed for enzyme catalysis, resulting in optimal transfer of chirality.

Conclusions

It can be concluded for this study that the dynamic binding differences and flexibility in binding of the Cu(II) complexes to DNA are the key parameters to achieve the highest ee and rate acceleration. The complexes which of them are more flexible in binding (i.e., **1** and **2**) to DNA are the best catalysts for DNA-based asymmetric Diels-Alder reaction. These structural findings are crucial to further structural studies to unravel the mechanism of chirality transfer in DNA-based asymmetric catalysis.

Experimental section

Salmon testes DNA (st-DNA) was obtained from Sigma and dialyzed against MOPS buffer (20 mM, pH 6.5) prior to use. The complexes $[Cu(dmbpy)(NO_3)_2]$ (1),[6] $[Cu(bpy)(NO_3)_2]$ (2),[6] $[Cu(phen)(NO_3)_2]$ (3),[6] $[Cu(dpq)(NO_3)_2]$ (5)[18] and $[Cu(dppz)(NO_3)_2]$ (6)[18] were prepared and isolated as reported previously. $[D_8]$-phenanthroline ($[D_8]$-phen), $[D_8]$-bipyridine ($[D_8]$-bpy) and $[D_{12}]$-dimethyl bipyridine ($[D_{12}]$-dmbpy) were prepared as reported previously.[34] Reagents obtained from commercial sources were used without further purification unless stated otherwise. Solvents for spectroscopic measurements were UVASOL (Merck) grade or better.

Synthesis of complexes $[D_{12}]$-dmbpy, **1**, **1a** and **4** and characterization by UV/Vis absorption, EPR, X-ray, IR and Raman spectroscopy can be found in ESI. For the experimental details, see ESI.

Catalysis was performed over a range of NaCl concentrations to determine its effect on the enantioselectivity of the reaction as described previously.[6] The apparent rate constants (k_{app}) were determined as described earlier.[5d]

Acknowledgements

Financial support is acknowledged from the European Research Council (ERC consolidator grant 279549, WRB), the Ubbo Emmius Fund of the University of Groningen (AD), the National Research School Catalysis (AB, GR) and from the Ministry of Education, Culture and Science (Gravity program 024.001.035, GR WRB).

Notes and references

Stratingh Institute for Chemistry, Faculty of Mathematics and Natural Sciences, University of Groningen, Nijenborgh 4, 9747 AG, Groningen, The Netherlands. Email: j.g.roelfes@rug.nl, w.r.browne@rug.nl.

† Electronic Supplementary Information (ESI) available: Details of synthesis and characterization of deuterated ligands and complexes, additional spectroscopic data. See DOI: 10.1039/b000000x/

1 F. Rosati, G. Roelfes, *ChemCatChem*, 2010, **2**, 916.
2 M. T. Reetz, *J. Org. Chem.,* 2009, **74**, 5767.
3 T. S. Koblenz, J. Wassenaar and J. N. H. Reek, *Chem. Soc. Rev.,* 2008, **37**, 247.
4 (a) J. C. Lewis, *ACS Catal.*, 2013, **3**, 2954; (b) T. Ueno, H. Tabe, and Y. Tanaka, *Chem. – An Asian J.*, 2013, **8**, 1646; (c) J. Oelerich and G. Roelfes, 'DNA-Based Metal Catalysis', in *Progress in Inorganic Chemistry*, *vol 57*, K.D. Karlin (Ed.), John Wiley & Sons, Inc., Hoboken, New Jersey, **2012**, pp. 353-393; (d) S. Park and H. Sugiyama, *Angew. Chem., Int. Ed.*, 2010, **49**, 3870; (e) T. R. Ward, *Acc. Chem. Res.*, 2010, **44**, 47.
5 (a) G. Roelfes and B. L. Feringa, *Angew. Chem. Int. Ed.,* 2005, **44**, 3230. (b) N. Shibata, H. Yasui, S. Nakamura, T. Toru, *Synlett,* 2007, 1153; (c) D. Coquière, B. L. Feringa and G. Roelfes, *Angew. Chem. Int. Ed.,* 2007, **46**, 9308; (d) A. J. Boersma, J. E. Klijn, B. L. Feringa and G. Roelfes, *J. Am. Chem. Soc.,* 2008, **130**, 11783; (e) A. J. Boersma, B. L. Feringa and G. Roelfes, *Angew. Chem. Int. Ed.,* 2009, **48**, 3346; (f) A. J. Boersma, D. Coquière, D. Geerdink, F. Rosati, B. L. Feringa and G. Roelfes, *Nat. Chem.,* 2010, **2**, 991; (g) A. J. Boersma, B. de Bruin, B. L. Feringa and G. Roelfes, *Chem. Commun.,* 2012, **48**, 2394. (h) S. Park, K. Ikehata, R. Watabe, Y. Hidaka, A. Rajendran and H. Sugiyama, *Chem. Commun.*, 2012, **48**, 10398; (i) R. P. Megens and G. Roelfes, *Chem. Commun.,* 2012, **48**, 6366; (j) J. Oelerich and G. Roelfes, *Chem. Sci.,* 2013, **4**, 2013; (k) J. Wang, E. Benedetti, L. Bethge, S. Vonhoff, S. Klussmann, J. Vasseur, J. Cossy, M. Smietana, and S. Arseniyadis, *Angew. Chem., Int. Ed.*, 2013, **52**, 11546. (l) Y. Li, C. Wang, G. Jia, S. Lu and C. Li, *Tetrahedron 2013*, **69**, 6585 (m) M. Wilking, U. Hennecke, *Org. Biomol. Chem.,* 2013, **11**, 6940.
6 G. Roelfes, A. J. Boersma and B. L. Feringa, *Chem. Commun.,* 2006, 635.
7 (a) K. E. Erkkila, D. T. Odom and J. K. Barton, *Chem. Rev.,* 1999, **99**, 2777; (b) C. Metcalfe and J. A. Thomas, *Chem. Soc. Rev.,* 2003, **32**, 215.
8 R. J. Errington, S. M. Ameer-beg, B. Vojnovic, L. H. Patterson, M. Zloh and P. J. Smith, *Advanced Drug Delivery Rev.,* 2005, **57**, 153.
9 (a) V. C. Pierre, J. T. Kaiser and J. K. Barton, *Proc. Natl. Acad. Sci. U.S.A.,* 2007, **104**, 429; (b) B. M. Zeglis, V. C. Pierre, J. T. Kaiser and J. K. Barton, *Biochemistry,* 2009, **48**, 4247; (c) S. N. Georgiades, and R. Vilar, *Annu. Rep. Prog. Chem. Sect. A.,* 2010, **106**, 481.
10 H. M. Berman and P. R. Young, *Annu. Rev. Biophys. Bioeng.,* 1981, **10**, 87.
11 (a) C. Hiort, B. Norden and A. Rodger, *J. Am. Chem. Soc.,* 1990, **112**, 1971; (b) D. Z. M. Coggan, I. S. Haworth, P. J. Bates, A. Robinson, A. Rodger, *Inorg. Chem.,* 1999, **38**, 4486.
12 M. Chikira, Y. Tomizawa, D. Fukita, T. Sugizaki, N. Sugawara, T. Yamazaki, A. Sasano, H. Shindo, M. Palaniandavar and W. E. Antholine, *J. Inorg. Biochem.,* 2002, **89**, 163.
13 (a) J. K. Barton, A. T. Danishefsky and J. M. Goldberg, *J. Am. Chem. Soc.,* 1984, **106**, 2172; (b) J. K. Arton, J. M. Goldberg, C. V. Kumar and N. J. Turro, *J. Am. Chem. Soc.,* 1986, **108**, 2081; (c) E. Tuite, P. Lincoln and B. Norden, *J. Am. Chem. Soc.,* 1997, **119**, 239.
14 (a) C. Cordier, V. C. Pierre and J. K. Barton, *J. Am. Chem. Soc.,* 2007, **129**, 12287; (b) S. S. David and J. K. Barton, *J. Am. Chem. Soc.,* 1993, **115**, 2984.
15 S. Satyanarayana, J. C. Dabrowiak and J. B. Chaires, *Biochemistry,* 1992, **31**, 9319.
16 (a) C. Hiort, B. Nordén and A. Rodger, *J. Am. Chem. Soc.,* 1990, **112**, 1971; (b) P. Lincoln and B. Nordén, *J. Phys. Chem. B*., 1998, **102**, 9583.
17 J. K. Barton, *Acc. Chem. Res.,* 1990, **23**, 273.
18 M. Navarro, E. J. Cisneros-Fajardo, A. Sierralta, M. Fernandez-Mestre, P. Silva, D. Arrieche and E. Marchan, *J. Biol. Inorg. Chem.,* 2003, **8**, 401.
19 B. J. Hathaway and D. E. Billing, *Coord. Chem. Rev.,* 1970, **5**, 143.
20 (a) J. Peisach and W. E. Blumberg, *Arch. Biochem. Biophys.,* 1974, **165**, 691; (b) U. Sakaguchi and A. W. Addison, *J. Chem. Soc. Dalton Trans.,* 1979, 600.
21 F. A. Walker and H. Sigel, *Inorg. Chem.*, 1972, **11**, 1162.
22 (a) H. Deng, A. Bloomfield, J. M. Benevides and G. J., Thomas, Jr. *Nucleic Acids Res*., 2000, **28**, 3379; (b) J. Ruiz-Chica, M. A. Medina, F. Sánchez-Jiménez and F. J. Ramírez, *Biochem. Biophys. Res. Commun.,* 2001, **285**, 437; (c) L. Pérez-Flores, A. J. Ruiz-Chica, J. G. Delcros, F. Sánchez-Jiménez and F. J. Ramírez, *J. Mol. Struc.,* 2005, 699; (d) C. A. Butler, R. P. Cooney and W. A. Denny, *Appl. Spectr.,* 1994, **48**, 822; (e) I. Chourpa and M. Manfait, *J. Raman Spect.,* 1995, **26**, 813; (f) J. C. Martin, R. M. Wartell and D. C. O'Shea, *Proc. Natl. Acad. Sci.,* 1978, **75**, 5483.
23 C. G. Coates, L. Jacquet, J. J. McGarvey, S. E. J. Bell, A. H. R. Al-Obaidi and J. M. Kelly, *J. Am. Chem. Soc.,* 1997, **119**, 7130.
24 W. Chen, C. Turro, L. A. Friedman, J. K. Barton and N. J. Turro, *J. Phys. Chem. B.,* 1997, **101**, 6995.
25 The band shifts are not attributable to optical phenomena, such as a change in the refractive index of the solution due to addition of st-DNA, since not all bands are shifted.
26 W. D. Wilson, C. R. Krishnamoorthy, Y. H. Wang and J. C. Smith, *Biopolymers,* 1985, **24**, 1941.
27 F.-A. Yang, C.-W. Guo, Y.-J. Chen, J.-H. Chen, S.-S. Wang, J.-Y. Tung, L.-P. Hwang and S. Elango, *Inorg. Chem.*, 2007, **46**, 578.
28 The lower S/N ratio in the EPR spectrum of **1** with excess NaCl might be either due to the poor glass quality or formation of anti-ferromagnetic coupled chlorido bridged Cu(II) dimers.
29 The changes possibly arise from coordination of the chloride anion to copper, since the affinity of chloride anion in water to copper(II) ion can be high ($pK_1 = 4$, $pK_2 = 4.7$, $pK_3 = 1.6$, $pK_4 = 0.17$).
30 A. Rodger and B. Norden, *Circular Dichroism and Linear Dichroism*, Oxford University Press, New York 1997.
31 M. Ardhammar, B. Nordén and T. Kurucsev, *DNA-Drug Interactions*, in *Circular Dichroism: Principles and Applications, Second Ed.*, N. Berova, K. Nakanishi and R.W. Woody, Editors. 2000, Wiley: New York.
32 G. Cohen and H. K. Eisenberg, *Biopolymers,* 1966, **4**, 429.
33 (a) L. Strekowski, J. L. Mokrosz, F. A. Tanious, R. A. Watson, D. Harden, M. Mokrosz, W. D. Edwards and W. D. Wilson, *J. Med. Chem.,* 1988, **31**, 1231; (b) H. M. Berman and P. R. Young, *Ann. Rev. Biophys. Bioeng.,* 1981, **10**, 87.
34 W. R. Browne, C. M. O'Connor, J. S. Killeen, A. L. Guckian, M. Burke, P. James, M. Burke and J. G. Vos, *Inorg. Chem.,* 2002, **41**, 4245.

Insight into the structure of DNA-based catalysts is obtained by elucidation of the DNA-binding mode of catalytically active copper complexes